C. R. Chimie 5 (2002) 89–98

S1631074802013279/FLA

Classical and non-classical iron hydrides: synthesis, NMR characterisation, theoretical investigation and X-ray crystal structure of the iron(IV) dihydride $[Cp^*Fe(dppe)(H)_2]^+BF_4^-$

Jean-René Hamon[a]*, Paul Hamon[a], Loïc Toupet[b], Karine Costuas[c], Jean-Yves Saillard[c]*

[a] *UMR CNRS 6509, Institut de chimie de Rennes, université de Rennes-1, Campus de Beaulieu, 35042 Rennes Cedex, France*
[b] *UMR CNRS 6626, université de Rennes-1, Campus de Beaulieu, 35042 Rennes cedex, France*
[c] *UMR CNRS 6511, Institut de chimie de Rennes, université de Rennes-1, Campus de Beaulieu, 35042 Rennes cedex, France*

Received 18 July 2001; accepted 28 August 2001

Abstract – Protonation of Cp*Fe(dppe)H (**1**; Cp* = η^5-C_5Me_5, dppe = $Ph_2PCH_2CH_2PPh_2$) by HBF_4Et_2O at –80 °C in diethylether affords the dihydrogen complex $[Cp^*Fe(dppe)(\eta^2\text{-}H_2)]^+BF_4^-$ ($\mathbf{2}^+BF_4^-$) in 90% yield. Its PF_6^- salt analogue ($\mathbf{2}^+PF_6^-$) is obtained in 94% yield by reaction between the 16-electron derivative $[Cp^*Fe(dppe)]^+PF_6^-$ ($\mathbf{3}^+PF_6^-$) with H_2 gas at –80 °C. The presence of a bound dihydrogen ligand in $\mathbf{2}^+$ is indicated by a short T_1 minimum values consistent with a H–H distances of 0.98(1) Å. For the partially deuterated derivative $\mathbf{2}^+$–d_1, the observed J_{HD} value of 27.0 Hz confirms the presence of the coordinated dihydrogen ligand, which displays an H–H separation of 0.97(1) Å, in complete agreement with the distance calculated using the T_1 static rotation model. Variable temperature NMR study shows the gradual, complete and irreversible transformation of the dihydrogen complex into its classical dihydride isomer *trans*-$[Cp^*Fe(dppe)(H)_2]^+$ ($\mathbf{4}^+$). Thermal solid state reaction (–20 °C, 48 h) of $\mathbf{2}^+BF_4^-$ gives quantitatively $\mathbf{4}^+BF_4^-$, whereas $\mathbf{4}^+PF_6^-$ is obtained by simple contact of H_2 with a solution of $\mathbf{3}^+PF_6^-$ in THF at room temperature. The crystal structure of $\mathbf{4}^+BF_4^-$ has been determined and shows a transoid arrangement of hydride ligands, consistent with the formulation of $\mathbf{4}^+$ as an iron(IV) dihydride. DFT calculations on both dihydride and dihydrogen isomers of $[Cp^*Fe(dppe)H_2]^+$ indicate that $\mathbf{4}^+$ is more stable than $\mathbf{2}^+$ by 0.19 eV, while this energy difference is reversed in the case of $[CpFe(dpe)H_2]^+$ (dpe = $H_2PCH_2CH_2PH_2$). The preference for the dihydride form in the case of $[Cp^*Fe(dppe)H_2]^+$ and of the dihydrogen one in the case of $[CpFe(dpe)H_2]^+$ is due to the larger π-donor and σ-acceptor abilities of the $[Cp^*Fe(dppe)]^+$ fragment, as compared to the $[CpFe(dpe)]^+$ unit. ***To cite this article: J.-R. Hamon et al., C. R. Chimie 5 (2002) 89–98*** © 2002 Académie des sciences / Éditions scientifiques et médicales Elsevier SAS

iron(IV) complexes / crystal structure / dihydrogen complexes / hydride complexes / DFT calculations

Résumé – La protonation du complexe hydrure Cp*Fe(dppe)H (**1**; Cp* = η^5-C_5Me_5, dppe = $Ph_2PCH_2CH_2PPh_2$) avec l'acide $HBF_4{\cdot}Et_2O$ à –80 °C dans l'éther éthylique conduit à la formation du complexe de l'hydrogène moléculaire $[Cp^*Fe(dppe)(\eta^2\text{-}H_2)]^+BF_4^-$($\mathbf{2}^+BF_4^-$) qui est isolé à basse température ($T < -50$ °C) sous la forme d'une poudre jaune citron avec un rendement de 90%. Son homologue sous forme de sel d'hexafluorophosphate ($\mathbf{2}^+PF_6^-$) est obtenu, avec un rendement de 94%, par réaction entre le dérivé à 16 électrons $[Cp^*Fe(dppe)]^+PF_6^-$ ($\mathbf{3}^+PF_6^-$) avec l'hydrogène gazeux à –80 °C. La présence d'un ligand dihydrogène coordonné au fer dans le complexe $\mathbf{2}^+$ est mis en évidence par un temps de relaxation longitudinal minimum (T_1) très court de 7 ms, en accord avec une distance H–H de 0,98(1) Å. La constante de couplage J_{HD} de 27,0 Hz, mesurée pour le composé partiellement deutérié $\mathbf{2}^+$–d_1, confirme la présence d'une molécule de H_2 coordonnée au métal dans le complexe $\mathbf{2}^+$ et permet de calculer une longueur de liaison H–H de 0,97(1) Å, en parfait accord avec la valeur obtenue en utilisant le modèle de rotation lente de la molécule d'hydrogène autour de l'axe Fe–H_2. L'étude en RMN du proton en température variable montre la transformation graduelle, totale et irréversible du complexe de l'hydrogène moléculaire en son isomère dihydrure *trans*-$[Cp^*Fe(dppe)(H)_2]^+$ ($\mathbf{4}^+$). Le complexe $\mathbf{4}^+BF_4^-$ est quantitativement obtenu par évolution thermique (–20 °C, 48 h) de $\mathbf{2}^+BF_4^-$ en phase solide, alors qu'un bullage d'hydrogène gazeux à température ambiante dans une solution de $\mathbf{3}^+PF_6^-$ dans le THF permet

* *Correspondence and reprints.*
E-mail addresses: jean-rene.hamon@univ-rennes1.fr (J.R. Hamon), saillard@univ-rennes1.fr (J.Y. Saillard).

d'isoler l'homologue $\mathbf{4}^{+}PF_6^{-}$ avec un rendement de 90%. La structure cristalline du composé $\mathbf{4}^{+}BF_4^{-}$ a été déterminée par analyse radiocristallographique et montre un arrangement transoïde des deux ligands hydrures, en accord avec une formulation du dérivé $\mathbf{4}^{+}$ comme une entité cationique de fer(IV) à 18 électrons. Des calculs DFT sur les isomères dihydrure et dihydrogène de $[Cp^*Fe(dppe)H_2]^{+}$ établissent que $\mathbf{4}^{+}$ est plus stable de 0,19 eV que $\mathbf{2}^{+}$. Cette différence d'énergie est inversée dans le cas de $[CpFe(dpe)H_2]^{+}$ (dpe = $H_2PCH_2CH_2PH_2$). La préférence pour la forme dihydrure dans le cas de $[Cp^*Fe(dppe)H_2]^{+}$ et pour la forme dihydrogène dans le cas de $[CpFe(dpe)H_2]^{+}$ est la conséquence du fait que le fragment $[Cp^*Fe(dppe)]^{+}$ est un meilleur donneur π et un meilleur accepteur σ que le fragment $[Cp^*Fe(dppe)]^{+}$. ***Pour citer cet article : J.-R. Hamon et al., C. R. Chimie 5 (2002) 89–98*** © 2002 Académie des sciences / Éditions scientifiques et médicales Elsevier SAS

complexes du fer(IV) / structure cristalline / complexes du dihydrogène / complexes dihydrure / calculs DFT

1. Introduction

Since the initial discovery by Kubas and co-workers of the transition metal dihydrogen complex $W(\eta^2\text{-}H_2)(P\mathit{i}Pr_3)_2(CO)_3$ [1,2], the chemistry of dihydrogen complexes has developed very rapidly, as manifested by a number of relevant reviews [2–8]. A large majority of these isolable dihapto-H_2 complexes has been found to be singly charged cationic species. This is mainly due to the common synthetic route of protonating a neutral metal hydride; an underlying aspect may be that the positive charge confers additional stability on the H_2 complexes [9–11]. While in this kind of compounds, monocationic ruthenium dihydride or dihydrogen complexes of the type $[Cp'RuH_2L_2]^{+}$ (Cp' = C_5H_5, C_5H_4R or C_5Me_5; L_2 = one diphosphine or two monodentate phosphine ligands) are common and their structures well established [12–15], their half-sandwich iron-based counterparts are scare. We have reported on the isolation and spectroscopic characterizations of the first half-sandwich organo-iron dihydrogen $[Cp^*Fe(dppe)(\eta^2\text{-}H_2)]^{+}$ ($\mathbf{2}^{+}$; Cp* = C_5Me_5, dppe = 1,2-bis(diphenylphosphino)ethane) [16]. It was obtained by protonation of Cp*Fe(dppe)H (**1**) with HBF_4 in Et_2O at –80 °C. The dihydrogen complex rearranges irreversibly into its tautomeric iron(IV) dihydride form *trans*-$[Cp^*Fe(dppe)(H)_2]^{+}$ ($\mathbf{4}^{+}$), as the temperature is raised. Two years later, Puerta and co-workers [17] published the synthesis and the X-ray crystal structure of another stable iron(IV) dihydride derivative *trans*-$[Cp^*Fe(dippe)(H)_2]BPh_4^{-}$ (dippe = 1,2-bis(diisopropylphosphino)ethane). The iron(IV) dihydride complex *trans*-$[CpFe(CO)(PEt_3)(H)_2]^{+}$ was also spectroscopically characterised at –78 °C by Brookhart and co-workers [18]. In this latter case, the dihydrogen compound is the thermodynamically more stable isomer.

On the other hand, steric interactions between the phosphine ligands and the C_5 ring associated with their respective electron richness have been established to play an important role in determining the position of the dihydrogen/dihydride equilibrium for ruthenium complexes [6,19]. However, such dihydride/dihydrogen equilibrium has not been observed in the case of related iron complexes. Nevertheless, a subtle balance of the steric and electronic environments around the metal is reached with the Cp*Fe(dppe) fragment that allows the isolation of both classical and non-classical dihydride isomers. Since the earlier theoretical studies on dihydrogen complexes [20,21], the electronic effects that govern the dihydride/dihydrogen equilibrium have been extensively investigated by various types of quantum chemical calculations [8,22]. It is generally admitted that strong π-donor metal centres tend to favour full dissociation of the H–H bond, i.e. to favour the dihydride form over the dihydrogen one. Therefore, the observation of both isomers requires a fine-tuning of the metal π-donor ability.

We report in this paper (*i*) full experimental details on the synthesis of both non-classical $[Cp^*Fe(dppe)(h^2\text{–}H_2)]^{+}X^{-}$ ($\mathbf{2}^{+}X^{-}$) and classical $[Cp^*Fe(dppe)(H)_2]^{+}X^{-}$ ($\mathbf{4}^{+}X^{-}$), cationic iron hydride complexes (X = BF_4, PF_6), (*ii*) NMR characterisation of the complexes, (*iii*) the X-ray crystal and molecular structure of the dihydride derivative *trans*-$[Cp^*Fe(dppe)(H)_2]^{+}BF_4^{-}$, and (*iv*) a theoretical analysis of the electronic structure of $\mathbf{2}^{+}$ and $\mathbf{4}^{+}$ by means of DFT calculations. A significant part of the experimental work has been reported in a preliminary form [16].

2. Experimental section

2.1. Materials

All manipulations were carried out under an argon atmosphere using Schlenk techniques. Reagent grade tetrahydrofuran (THF), diethyl ether and pentane were dried and distilled from sodium benzophenone ketyl prior to use. Dichloromethane and acetone were distilled under argon from P_2O_5 and B_2O_3, respectively. Complexes Cp*Fe(dppe)H [23], Cp*Fe(dppe)D [23] and $[Cp^*Fe(dppe)]^{+}PF_6^{-}$ [24] were prepared following the published procedures, and other chemicals were purchased from commercial sources and used as

received. NMR spectra were recorded on multinuclear Bruker AM300WB (300 MHz) or DPX 200 (200 MHz) spectrometers. Chemical shifts are reported (in ppm) relative to internal tetramethylsilane (TMS) or to the residual proton resonance resulting from incomplete deuteration of the NMR solvents for ^{1}H NMR; the carbon of the deuterated NMR solvents for ^{13}C NMR; external 85% H_3PO_4 for ^{31}P NMR, and external $CFCl_3$ for ^{19}F NMR. Proton T_1 studies were performed using the standard inversion recovery 180°–τ–90° pulse sequence method [25]. Temperatures within the NMR probe were controlled by a Bruker VT unit, and temperature calibration was accomplished by following the Van Geet methanol calibration method [26], and found to be accurate within 1 °C. The samples for variable-temperature NMR were prepared in degassed CD_2Cl_2 in 5 mm NMR tubes. Elemental analyses were performed at the Centre for Microanalyses of the CNRS at Vernaison, France.

2.2. Synthesis and characterisation

*2.2.1. [Cp * Fe(dppe)(η^2-H_2)]$^+BF_4^-$ ($2^+BF_4^-$)*

To a cooled (–80 °C) orange diethylether solution (20 ml) of 0.59 g (1.0 mmol) of Cp*Fe(dppe)H were added by syringe 187 µl (1.5 mmol) of $HBF_4{\cdot}OEt_2$. A yellow suspension formed and the stirring is maintained for 3 h. The solid was filtered off, washed with cold pentane (4 × 50 ml), and dried under vacuum at temperature always below –50 °C. Complex [Cp*Fe(dppe)(η^2-H_2)]$^+BF_4^-$is isolated as a lemon–yellow powder in 95% yield (0.64 g). ^{1}H NMR (300 MHz, CD_2Cl_2, 193 K) δ: 7.96–7.39 (m, 20 H, Ph), 2.07–1.92 (2m, 4 H, CH_2), 1.45 (s, 15 H, C_5Me_5), –12.39 (bs, $w_{1/2}$ = 50 Hz, 2 H, Fe(η^2-H_2); T_1 min (223 K, 300 MHz) = 7 ms). ^{13}C NMR (75 MHz, CD_2Cl_2, 193 K) δ: 136.5–129.1 (m, Ph), 91.1 (s, C_5Me_5), 31.1 (m, CH_2, J_{CH} = 136 Hz), 10.1 (q, C_5Me_5, J_{CH} = 128 Hz). ^{31}P NMR (121 MHz, CD_2Cl_2, 193 K) δ: 93.6 (s, dppe).

*2.2.2. [Cp * Fe(dppe)(η^2-H_2)]$^+PF_6^-$ ($2^+PF_6^-$)*

A Schlenk tube under argon, containing a cooled (–80 °C) THF solution (30 ml) of [Cp*Fe(dppe)]$^+PF_6^-$ (0.734 g, 1.0 mmol), is pressurised with 2 bar of H_2. The initial orange–red color of the solution turned immediately yellow and the stirring is continued for 15 min. Low temperature work up, as described above, provided 0.662 g (90% yield) of [Cp*Fe(dppe)(η^2-H_2)]$^+PF_6^-$, authenticated by comparison of its ^{1}H NMR data with those of its corresponding BF_4^- salt (see § **2.2.1.**).

*2.2.3. [Cp * Fe(dppe)$(H)_2$]$^+BF_4^-$ ($4^+BF_4^-$)*

A yellow solid sample of [Cp*Fe(dppe)(η^2-H_2)]$^+BF_4^-$ (0.405 g, 0.6 mmol), prepared as described above in § **2.2.1.**, was kept in a Schlenk tube under argon, at 20 °C for 48 h. The colour of the solid material turned light orange–yellow. The solid is dissolved in 10 ml of acetone. The solution is filtered off, concentrated to 2 ml and layered with 10 ml of pentane. A yellow–orange precipitate formed. After filtration and drying under vacuum, 0.381 g (94%) of [Cp*Fe(dppe)$(H)_2$]$^+BF_4^-$ are recovered as air and thermally stable microcrystals. Anal. calcd for $C_{36}H_{41}BFeF_4P_2$: C, 63.75%; H, 6.09%; P, 9.13%. Found: C, 63.39%; H, 5.85%; P, 9.22%. ^{1}H NMR (200 MHz, CD_3COCD_3) δ: 8.01–7.35 (m, 20 H, Ph), 2.33 (m, 2 H, CH_2), 2.27 (m, 2H, CH_2), 1.58 (s, 15 H, C_5Me_5), –7.65 (t, 2 H, Fe-H, J_{HP} = 69 Hz). ^{13}C {^{1}H} NMR (50 MHz, CD_3COCD_3), δ: 135.3 (t, Ph), 131.8 (s, Ph), 129.6 (t, Ph), 96.1 (s, C_5Me_5), 33.7 (t, CH_2), 9.8 (s, C_5Me_5). ^{31}P NMR (81 MHz, CD_3COCD_3), δ: 90.8 (t, dppe, J_{PH} = 69 Hz). ^{19}F NMR (188 MHz, CD_3COCD_3) δ: 127.0 (BF_4^-).

*2.2.4. [Cp*Fe(dppe)$(H)_2$]$^+PF_6^-$ ($4^+PF_6^-$)*

A Schlenk tube under argon, containing a THF solution (30 ml) of [Cp*Fe(dppe)$^+PF_6^-$ (0.734 g, 1.0 mmol), is pressurised with 2 bar of H_2. The initial orange color of the solution turned immediately yellow and the stirring is continued for 5 min. The solvent is then evaporated under reduced pressure and the yellow residue is washed with pentane (3 × 20 ml). Following the extraction with dichloromethane, concentration of the extracts, filtration and precipitation with an excess of diethyl ether, 0.660 g (90% yield) of [Cp*Fe(dppe)$(H)_2$]$^+PF_6^-$ are isolated, and identified by comparison of its ^{1}H NMR parameters with those of its corresponding BF_4^- salt (see § **2.2.3.**).

2.3. Crystallographic data collection and refinement of the structure of $4^+BF_4^-$

X-ray quality crystals of [Cp*Fe(dppe)$(H)_2$]$^+BF_4^-$ were grown as described above in § 2.2.3. section. Diffraction data were collected at 293 K with an Enraf-Nonius CAD-4 diffractometer, using graphite monochromated MoK_α radiation (λ = 0.710 69 Å). Crystal parameters and refinement results are summarised in Table 1. Complete details of the crystal data, X-ray data collection, and structure solution are provided as Supporting Information. Cell constants and orientation matrix for data collection were obtained from a least-squares refinement using 25 high-θ reflections. After Lorenz and polarisation corrections [27], the structure was solved with SIR-97 [28], which revealed all non-hydrogen atoms of the molecule. A riding model was applied to hydrogen atoms bound to carbon (C–H = 0.96 Å), which were included in the model at idealised positions, while hydrogen atoms bound to iron were located in Fourier

difference maps and were not refined. Isotropic thermal parameters were considered for all H-atoms equal to 1.2 times the equivalent isotropic thermal parameters of the corresponding parent atom. The whole structures were next refined with SHELXL97 [29], by the full-matrix least-square techniques based on F^2, including all reflections. Atomic scattering factors were taken from the literature [30]. The refinements converged at conventional *R*-factors of 0.0677, for 3045 reflections with $I > 2\,\sigma(I)$ ($R = 0.1916$ for all reflections). ORTEP view of the molecule (Fig. 1) was generated with PLATON98 [31]. All the calculations were performed on a Pentium NT Server computer.

2.4. Computational details

DFT calculations [32–35] were carried out using the Amsterdam Density Functional (ADF) program [36]. The Vosko–Wilk–Nusair parameterisation [37] was used to treat electron correlation within the local density approximation (LDA). The non-local corrections of Becke [38,39] and of Perdew [40,41] were added to the exchange and correlation energies, respectively. The numerical integration procedure applied for the calculations was developed by te Velde et al. [35] A triple-ζ Slater-type orbital (STO) basis set was used for Fe 3d and 4s, and a single-ζ STO was used for Fe 4p. Concerning the hydrogen atoms directly bonded to the Fe centre, a triple-ζ STO basis set was employed for 1s, augmented with a single-ζ polarization function 2p. The other atoms were described by a double-ζ STO basis set for H 1s, C 2s and 2p, and P 3s and 3p, augmented with a single-ζ polarization function (2p for H, C; 3d for P). Full geometry optimisations (assuming a C_1 symmetry) were carried out on each complex, using the analytical gradient method implemented by Verluis and Ziegler [42]. A DFT fragment analysis, which includes a fragment MO population decomposition, was also made on each complex in the way proposed by Ziegler and co-workers [43–45].

Table 1. Crystal data, data collection, and refinement parameters for complex *trans*-[Cp*Fe(dppe)$(H)_2]^+BF_4^-$ (**4**$^+BF_4^-$).

Formula	$C_{36}H_{41}BF_4FeP_2$
FW	678.29
Temperature (K)	293(2)
Crystal system	monoclinic
Space group	$P2_1/c$
a (Å)	11.838(6)
b (Å)	13.216(9)
c (Å)	22.186(12)
α (°)	90
ß (°)	103.21(2)
γ (°)	90
V (Å^3)	3379(3)
Z	4
$D_{(calcd)}$ (g cm^{-3})	1.333
Crystal size (mm)	0.35 × 0.32 × 0.25
F(000)	1416
Diffractometer	CAD4
Radiation *λ*	0.710 69
Absorption coefficient (mm^{-1})	0.587
θ range (°)	1.77–24.98
Range *h*,*k*,*l*	0/14, 0/15, –26/26
Number of total reflections	6234
Number of unique reflections	5927
Number of observed reflections [$I > 2\,\sigma$(I)]	3045
Restraints/parameters	0/398
$\omega = 1/[\sigma^2 (F_o)^2 + (a\,P)^2 + b\,P]$	*a* = 0.1470
(where $P = [F_o^2 + 2\,F_c^2]/3$)	*b* = 0.0000
Final *R*	0.0677
R_ω	0.1747
R indices (all data)	0.1916
R_ω (all data)	0.2252
Goodness of fit / F^2	0.962
Largest diffraction peak & hole (e Å^{-3})	0.537 –0.763

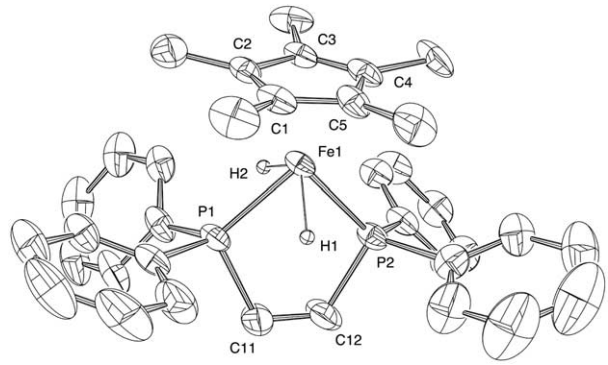

Fig. 1. ORTEP view of the *trans*-[Cp*Fe(dppe)$(H)_2]^+$ cation. Hydrogen atoms (except the hydrides) and BF_4^- anion are omitted for clarity. Thermal ellipsoids are plotted at the 50% probability level.

3. Results and discussion

3.1. Preparation and spectroscopic characterisations of complexes

Protonation of the thermally stable neutral hydride derivative Cp*Fe(dppe)H (**1**) [23] by a slight excess (1.5 equiv) of $HBF_4{\cdot}Et_2O$ in diethyl ether at –80 °C affords rapidly the corresponding cationic dihydrogen complex [Cp*Fe(dppe)(η^2-H_2)]$^+BF_4^-$ (**2**$^+BF_4^-$), isolated in 95% yield as a lemon-yellow powder after work up at low temperature ($T < -50$ °C) (Fig. 2). Its PF_6^- salt dihydrogen analogue **2**$^+PF_6^-$ was prepared in 90% yield by stirring a THF solution of the paramagnetic red 16-electron iron(II) complex [Cp*Fe(dppe)]$^+PF_6^-$ (**3**$^+PF_6^-$) [24] under H_2 (2 atm) at –80 °C (Fig. 2). Despite their thermal instability, solid samples of **2**$^+$ can be stored for several weeks under argon at low temperature, without any signs of decomposition.

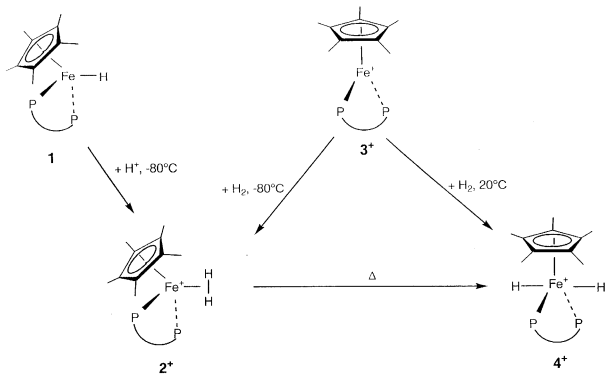

Fig. 2. Reactional route from **1** to **4**$^+$.

In the hydride region of its ^{1}H NMR spectrum (CD_2Cl_2, 193 K), complex **2**$^+$ displayed a broad resonance at δ –12.39, which integrated for 2 protons. The relaxation time of the metal bound hydride (300 MHz, shows a minimum of T_1 (longitudinal relaxation time) of 7 ms at 223 K, in agreement with the formulation of complex **2**$^+$ as a dihydrogen derivative.

The HD complex [Cp*Fe(dppe)(η^2-HD)]BF_4 (**2**$^+$-$d_1BF_4^-$ was correspondingly prepared by protonation of the neutral iron deuteride Cp*Fe(dppe)D [23] with $HBF_4{\cdot}Et_2O$. The expected 1:1:1 triplet centred at δ –12.4 was observed for **2**$^+$-$d_1BF_4^-$, and the value of $J_{H–D}$ was determined to be 27.0 Hz, which is diagnostic of an η^2-H_2 bonding interaction and unequivocally establishes the structure of **2**$^+BF_4^-$.

Using the correlation established by Morris et al. [46] or that of Luther and Heinekey [47], it is possible to estimate the H–H distance knowing the H–D coupling within a dihydrogen complex. The value obtained in our case is 0.97 ± 0.01 Å, in good agreement with calculations (see below). Evaluation of the H–H distance within the dihydrogen complex can also be achieved using relaxation data [48]. Depending upon the relative rate of the H_2 ligand rotation around the M–H_2 axis, two possible values for the H–H distance can be calculated from the T_1 minimum values using static and fast-rotation models [6,49,50]. The determination of the H–H bond lengths in the H_2 ligand of the cation **2**$^+$ by the T_1 minimum method using a static rotation model afforded an H–H separation of 0.98 ± 0.01 Å, a value very close to that calculated from the J_{HD} value (0.97 Å). This distance is in agreement with the presence of a slightly stretched dihydrogen ligand in the coordination sphere of iron, due to the electron-releasing capabilities of the cationic organometallic moiety, and fully consistent with the theoretical results (see § **3.3.**).

Upon warming, the dihydrogen complex **2**$^+$ converts, either in solution or in the solid state, to its respective *trans*-classical dihydride isomer [Cp*Fe(dppe)$(H)_2$]$^+$ (**4**$^+$), as its BF_4^- or PF_6^- salt, which is the exclusive product at room temperature (Fig. 2). Thus, pure dihydride complex **4**$^+BF_4^-$ is isolated in 94% yield after keeping a sample of the dihydrogen complex **2**$^+BF_4^-$ under argon at –20 °C for two days. On the other hand, complex **4**$^+PF_6^-$ is prepared in quantitative yield by simple exposure of the 16-electron derivative **3**$^+PF_6^-$ to H_2 gas, at room temperature (Fig. 2).

The dihydrogen/dihydride transformation in solution upon warming is cleanly followed by 1H NMR spectroscopy, which reveals the appearance and the progressive increase of a sharp triplet at –7.65 ppm with the concomitant decrease and eventually complete disappearance of the broad resonance at –12.39 ppm. If the sample is cooled again to –80 °C, no dihydrogen complex reforms, which indicates that the process is gradual, complete, and irreversible, the classical dihydride complex being the thermodynamically more stable isomer.

The **4**$^+$ salts are yellow–orange crystalline materials, which are non-air- or moisture-sensitive. The IR spectra do not show bands clearly attributable to ν(FeH). As stated above, the hydridic protons of an isolated species **4**$^+$ appear on the ^{1}H NMR spectrum in acetone-d_6 as a triplet centred at –7.65 ppm due to coupling (J_{HP} = 69 Hz) with two equivalent phosphorus nuclei. One singlet is observed at δ 90.8 on the $^{31}P\{^1H\}$ NMR spectrum, which transforms in a triplet with J_{PH} = 69 Hz in the undecoupled spectrum. These data suggest the equivalence of the hydride ligands and the two phosphorus atoms. The classical dihydride structure for **4**$^+BF_4^-$ is supported by the relaxation time $T_{1\,min}$ = 175 ms (300 MHz, acetone-d_6, 223 K), which rules out any bonding interaction between the hydrides. According to these data, compounds **4**$^+$ must have four-legged piano stool structure. The transoid disposition (C_{2v} symmetry), with two orthogonal mirror planes (assuming free rotation of the C_5Me_5 ligand), can be confidently attributed on the basis of the simplicity of the $^{13}C\{^1H\}$ NMR spectrum. Indeed, all four phenyl groups are equivalent and give rise to three separate resonances for the four magnetically non-equivalent carbon atoms of these phenyl groups. This pattern, which is probably due to accidental degeneracy of two signals, clearly indicates a change from the C_s symmetry, invariably observed for the three-legged piano stool structure of previous compounds in this series [23,51,52] to a C_{2v} symmetry.

These results sharply contrast with those of Brookhart et al. [18], in which the opposite situation was observed. The in-situ generated dihydrogen complexes [CpFe(CO)L(η^2-H_2)]BAr'$_4$ (Cp = C_5H_5; L = PEt_3, PPh_3; Ar' = 3,5-$(CF_3)_2(C_6H_3)$ are indeed the thermodynami

cally more stable isomers. The classical *trans*-dihydride derivative (L = PEt_3) was however, characterized at –78 °C by ^1H NMR spectroscopy, and no equilibrium between the dihydride and the dihydrogen forms was found. The $[Cp^*Fe(dppe)]^+$ metal centre is more electron-rich than that in the $[CpFe(CO)L]^+$ moiety, thus favouring the oxidative addition of coordinated H_2 through an increase back bonding in the σ* orbital of the dihydrogen ligand. This electronic difference is also illustrated in the J_{HD} value that is equal to 32 Hz in Brookhart's compound [18] and is consistent with a loose binding of H_2 to the metal centre, as compared to the 27 Hz value found in our case. A rapid equilibrium has however been reported in this series of piano-stool structure Cp*Fe complexes [53]. It occurs between the classical highly fluxional and unstable iron(IV) trihydride complex $Cp^*FeH_3(PMe_3)$, generated only in benzene or tetrahydrofuran solution, and its non-classical Fe(II) dihydrogen-hydride form $Cp^*FeH(\eta^2\text{-}H_2)(PMe_3)$ as deduced from J_{HD} and minimum T_1 measurements. Steric protection must then play an important role in stabilizing trans-dihydride iron(IV) compounds. Complex $[Cp^*Fe(dmpe)(H)_2]^+BF_4^-$ (dmpe = 1,2-bis(dimethylphosphino)ethane), which was obtained by protonation of its corresponding monohydride precursor, was found to be extremely unstable in solution [53], whereas the homologue complexes, bearing bulkier diphosphines dppe and dippe, $[Cp^*Fe(dppe)(H)_2]^+$ (**4**$^+$) and $[Cp^*Fe(dippe)(H)_2]^+BPh_4^-$ [17] are isolated at room temperature. On the other hand, coordination of dihydrogen or its homolytic splitting at metal centre greatly depends on the electron-donating capabilities of the organometallic moieties [8,20,21]. Thus, when the chelating diphosphine ligand dppe is substituted for the dippe (a better σ-donor but poorer π-acceptor than the dppe) at the iron centre, Puerta et al. have reported that the stabilisation of coordinated dihydrogen is no more possible with the very electron-rich fragment $[Cp^*Fe(dippe)]^+$ [17], whereas the dihydrogen complex **2**$^+$ is isolated at low temperature. This is in accord with the criterion for the stability of the metal–dihydrogen bond proposed by Morris, based upon the value of $\nu(N_2)$ for the associated dinitrogen complex [54]. The $[Cp^*Fe(dppe)]^+$ fragment adds N_2 to provide the end-on dinitrogen complex $[Cp^*Fe(dppe)(N_2)]^+$ [55], which exhibits a strong N–N stretching vibration at 2117 cm^{-1}, whereas the $[Cp^*Fe(dippe)]^+$ complex is reluctant to N_2 coordination.

3.2. X-ray crystal structure determinations of *trans*-$[Cp^*Fe(dppe)(H)_2]^+BF_4^-$ ($4^+BF_4^-$)

The X-ray crystal structure of $\mathbf{4}^+BF_4^-$ has been determined as outlined in the 'Experimental' section, confirming its formulation as a classical organo-iron(IV) dihydride. A view of the molecular structure of the organometallic cationic moiety $[Cp^*Fe(dppe)(H)_2]^+$ is presented in Fig. 1. Relevant interatomic distances and angles are listed in Table 2. The two hydrides were located but not refined, and as such this does not provide accurate structural information. More reliable data on the bonding within the FeH_2 fragment are provided by solution ^1H and ^{31}P NMR experiments (vide supra). However, the coordination around iron can be unambiguously described as a distorted four-legged piano stool structure. The two hydride atoms are in transoid positions, with an H(1)–Fe(1)–H(2) angle of 110.5°, and the plane containing these three atoms makes an angle of 76.1° with the plane of the C_5 ring. The iron–hydride bond distances Fe(1)–H(1) 1.48 Å and Fe(1)–H(2) 1.50 Å are in the normal range previously measured in other iron(IV) hydride complexes, with Fe–H distances ranging from 1.1(1) to 1.72(9) Å [17,56–60]. One can note however, that in the closely related bis(diisopropylphosphino)ethane derivative $[Cp^*Fe(dippe)(H)_2]^+BPh_4^-$, the iron–hydride bond distances are somewhat shorter 1.35(6) and 1.41(5) Å [17].

The other bond lengths show interesting trends. The Fe–P separations (2.166(2) and 2.170(2) Å) are the shortest never measured for complexes possessing the 'Cp*Fe(dppe)' framework (range 2.20–2.31 Å) [23,24 51,52,61]. The C_5Me_5 group is planar and the Fe–Cp* centroid distance (1.728(6) Å) is also significantly shorter than usually observed (av 1.76 Å) for neutral and cationic iron species in this series [23,24,51,52,61]. This Fe–P and Fe–C bond shortening can be attributed to the contraction of the Fe radius upon increase of the oxidation state from +II to +IV. Such an ionic radius effect has already been noticed in other systems [52, 62]. The bite angle P(1)–Fe(1)–P(2) of 90.73(8)° matches perfectly the calculated value (90.8°) (vide infra), and is identical to that reported for the dippe analogue (90.67(9)°) [17]. The plane containing the iron and the two phos

Table 2. Selected bond lengths (Å) and angles (°) for complex *trans*-$[Cp^*Fe(dppe)(H)_2]^+BF_4^-$ ($\mathbf{4}^+BF_4^-$).

Bond distances

Fe(1)–Cp^*_{CNT} [a]	1.728(6)	Fe(1)–C(Cp^*) [b]	
Fe(1)–P(1)	2.170(2)	Fe(1)–C(1)	2.084(6)
Fe(1)–P(2)	2.166(2)	Fe(1)–C(2)	2.103(6)
Fe(1)–H(1)	1.48	Fe(1)–C(3)	2.122(6)
Fe(1)H(2)	1.50	Fe(1)–C(4)	2.116(6)
Fe(1)–C(1–5) av.	2.104(6)	Fe(1)–C(5)	2.097(6)

Bond angles

P(1)–Fe–P(2)	90.73(8)	H(1)–Fe(1)–H(2)	111
P(1)–Fe(1)–H(1)	62	P(1)–Fe(1)–H(2)	59
P(2)–Fe(1)–H(1)	61	P(2)–Fe(1)–H(2)	86
Cp^*_{CNT}–Fe(1)–P(1)	135.3	Cp^*_{CNT}–Fe(1)–P(2)	133.9
Cp^*_{CNT}–Fe(1)–H(1)	132	Cp^*_{CNT}–Fe(1)–H(2)	116

[a] Abbreviations: Cp* = C_5Me_5; CNT = centroid. [b] Average value.

phorus atoms is almost perpendicular (87.4°) to the plane of the C_5 ring, as we have previously reported for the 16-electron Fe(II) complex $3^+PF_6^-$ (84.8°) [24], and for the 17-electron iron(III) deuteride radical cation $[Cp^*Fe(dppe)D]^+$ (88.8°) [16]. All the other bond lengths and angles measured in the ligands and tetrafluoroborate anion are unexceptional.

Iron(IV) still remains relatively uncommon. This unusual oxidation state is found in coordination compounds containing donor nitrogen [63–65] and sulfur ligands [66–68]. A mixed inorganic/organometallic cationic Fe(IV) derivative $[Cp^*Fe(\eta^2\text{-}S_2CNMe_2)_2]PF_6$ has been isolated by Desbois and Astruc [69]. The organometallic complex $Fe(norbornyl)_4$ is also known [70], but as far as iron hydrides are concerned, the formal +IV oxidation state is still very unusual. The other reliably established Fe(IV) hydride systems are the neutral bis-trichlorosilyl monohydride $CpFe(CO)H(SiCl_3)_2$ [71,72], the cationic dihydride $[Cp^*Fe(dippe)(H)_2]^+$, obtained by reaction of H_2 with the 16-electron compound $[Cp^*Fe(dippe)]^+$ [17], and the series of neutral dihydride *trans*-$(\eta^6$-arene$)Fe(H)_2(SiRX_2)_2$ complexes (arene = benzene, toluene, *p*-xylene; R = Cl, F, H, Me; X = Cl, F) resulting from oxidative addition of $HSiRX_2$ at arene-solvated iron atoms [56–59]. The crystal structure of the thermally stable and fluxional cationic trihydride derivative $[FeH_3(PEt_3)_4][BAr'_4]$ (Fe–H av. = 1.44(7) Å) has recently been reported by Berke and co-workers [60]. The same structure, assumed on spectroscopic grounds, was also reported for the neutral hydrido-stannyl complex $FeH_3(PPh_2Et)_3(SnPh_3)$ [73]. Its C_3 symmetric heavy atom skeleton and the fact that the metal-bound hydrogens were not located are reminiscent of the '$Fe(PEt_3)_4$' core of Berke's cationic trihydride [60].

3.3. Theoretical investigations

In order to provide a rationalisation of the structure and bonding of the title compound and to provide a comparison between its dihydride and dihydrogen forms, we have carried out DFT calculations, firstly on the simplified model $[CpFe(dpe)H_2]^+$ (dpe = $H_2PCH_2CH_2PH_2$). Two stable conformations were found, corresponding to the hydrogen atoms lying in the trans and cis positions, respectively. The corresponding optimised structures are shown in Fig. 3. Their major metrical data are given in Table 3. Both geometries are close to the ideal C_s symmetry, which cannot be perfectly reached because of the slight distortion out of planarity of the PCCP diphosphine framework. The trans conformation corresponds to a dihydride form and its geometry is very similar to that found in the X-ray structure of **4**$^+$ (Fig. 1). The cis conformation is the dihydrogen form $[CpFe(dpe)(\eta^2\text{-}H_2)]^+$, with an H–H distance of 0.900 Å. The cis dihydrogen form is calculated to be more stable than its trans dihydride isomer by 0.19 eV. The search for other minima on the potential energy surface of $[CpFe(dpe)H_2]^+$ was unsuccessful, strongly suggesting that only the two optimised trans and cis geometries are stable conformations of $[CpFe(dpe)H_2]^+$. In particular, there is no trans or

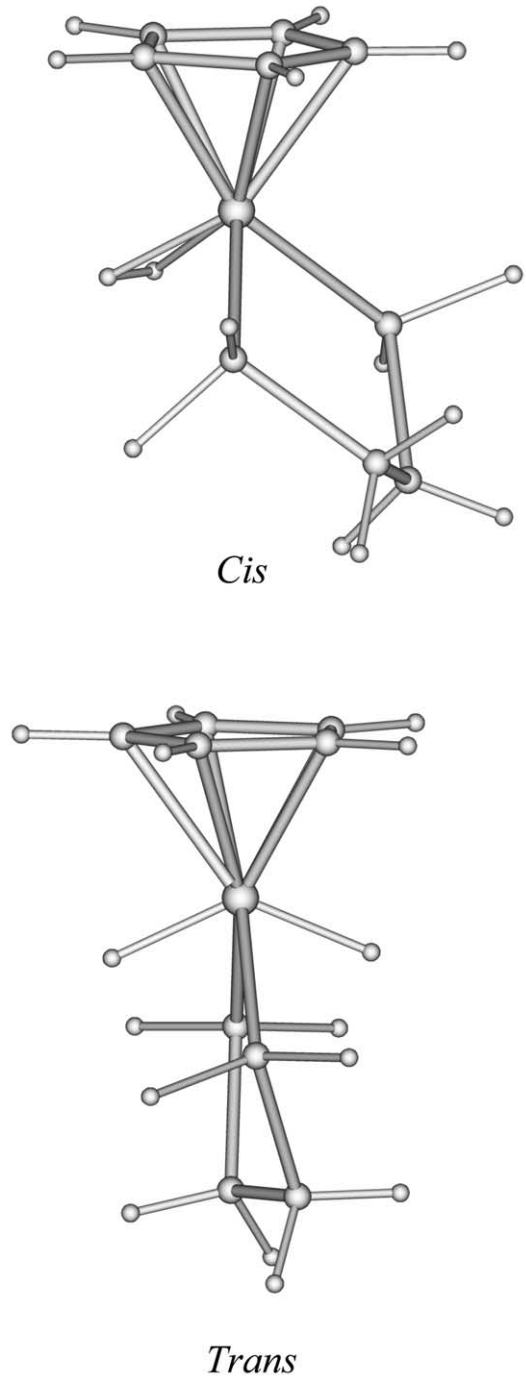

Fig. 3. Optimised geometries of the *cis*- and *trans*- isomers of $[CpFe(dpe)H_2]^+$.

Table 3. Relative energies and major structural data of the optimised geometries of the *cis*- and *trans* isomers of $[CpFe(dpe)H_2]^+$ and $[Cp^*Fe(dppe)H_2]^+$.

	cis-$[CpFe(dpe)H_2]^+$	**trans-$[CpFe(dpe)H_2]^+$**	**cis-$[Cp^*Fe(dppe)H_2]^+$**	**trans-$[Cp^*Fe(dppe)H_2]^+$**
Relative energy between the *cis* and *trans* isomers (eV)	0.000	0.187	0.190	0.000
Fe–H(1)	1.600	1.514	1.564	1.515
Fe–H(2)	1.593	1.512	1.569	1.510
H(1)–H(2)	0.900	2.764	0.935	2.733
Fe–P	2.221–2.222	2.191–2.190	2.255–2.259	2.202–2.207
$Fe–C(Cp)_{range}$	2.117–2.138	2.098–2.132	2.127–2.214	2.126–2.172
$Fe–C(Cp)_{av.}$	2.129	2.117	2.170	2.149
$Cp_{centroid}$–Fe–(middle of P···P)	143.2	178.7	150.8	178.8
P–Fe–P	85.3	90.65	86.2	90.8
P–Fe–H(1)	81.9–105.5	71.6–73.6	77.9–98.3	72.0–72.8
P–Fe–H(2)	103.0–82.6	73.1–73.6	105.7–79.7	74.5–70.50
H(1)–Fe–H(2)	32.7	131.9	34.7	129.2
$Cp_{centroid}$–Fe–H(1)	120.0	114.2	114.6	114.2
$Cp_{centroid}$–Fe–H(2)	121.5	113.8	119.9	116.6
$Cp_{centroid}$–Fe–P	126.2–126.0	133.8–135.6	131.5–127.6	134.6–134.6
P–P–C–C (dppe or dpe)	25.5	25.1	28.1	24.6

transoid stable dihydrogen form, neither cis nor cisoid stable dihydride form. This result showing the existence of two isomers lying close in energy, the cis dihydrogen form being the most stable, is comparable to that found experimentally by Brookhart et al. on the closely related $[Cp(CO)(PEt_3)H_2]^+$ compound [18]. The Fe–P and Fe–C(Cp) distances are shorter in trans-$[CpFe(dpe)(H)_2]^+$ than in cis-$[CpFe(dpe)(\eta^2\text{-}H_2)]^+$. This can be attributed to the change in the metal oxidation state when going from the dihydride to dihydrogen isomers (Fe(IV) to Fe(II)) and therefore to the concomitant increase of the atomic radius (vide supra).

Since the dihydrogen form of the $[CpFe(dpe)H_2]^+$ model was found to be slightly more stable than its dihydride isomer, and that only the dihydride form of $[Cp^*Fe(dppe)H_2]^+$ is isolated at room temperature, we decided to carry out DFT calculations on the real $[Cp^*Fe(dppe)H_2]^+$ compound, in the same manner as we did for the $[CpFe(dpe)H_2]^+$ model. Similarly, two minima were identified, a *trans*- dihydride (**4**$^+$) and a *cis* dihydrogen (**2**$^+$) complex. Their structure, not shown here, looks very much the same as those of $[CpFe(dpe)H_2]^+$ (Fig. 3). Their major structural parameters are given in Table 3. Nevertheless, some differences between the $[CpFe(dpe)H_2]^+$ and $[Cp^*Fe(dppe)H_2]^+$ structures can be noticed. Comparing both *cis*-isomers, $[Cp^*Fe(dppe)(H_2)]^+$ has longer Fe–P and Fe–C(Cp) distances. Similarly, its H–H distance is longer (0.935 Å), while its Fe–H distances are shorter. These differences suggest a stronger π-donor ability of the $[Cp^*Fe(dppe)]^+$ unit, as compared to its hypothetical $[CpFe(dpe)]^+$ homologue. Stronger π back-donation into the H_2 σ*(H_2) orbital reinforces the Fe–H bonds and concomitantly weakens the H–H bond [8]. On the other hand, this effect occurs at the expense of π back-donation toward the other ligands, thus weakening their bonding to the metal. In fact, it is possible to get a better insight into the comparison of the bonding abilities of the $[CpFe(dpe)]^+$ and $[Cp^*Fe(dppe)]^+$ units in carrying out a DFT fragment analysis of $[CpFe(dpe)(\eta^2\text{-}H_2)]^+$ and **2**$^+$ [43–45]. The bonding energy between dihydrogen and the metallic unit is 1.481 and 1.495 eV in the former and the latter respectively. The stronger bond in the case of **2**$^+$ is due to a larger electron transfer into the σ(H_2) orbital (0.22 vs 0.17 electron), but also to a larger donation to the metal by the σ(H_2) orbital whose population is lower in the case of **2**$^+$ (1.59 vs 1.66 electron). Clearly, $[Cp^*Fe(dppe)]^+$ is a better π-donor and a better σ-acceptor than $[CpFe(dpe)]^+$. If they are strong enough, both effects, especially the second one, tend to favour full dissociation of the H–H bond, i.e. to favour the dihydride form over the dihydrogen one [8,20,21] This is exactly what happens in the case of $[Cp^*Fe(dppe)H_2]^+$, for which, contrary to $[CpFe(dpe)H_2]^+$, the *trans* dihydride isomer is calculated to be more stable than the *cis* dihydrogen one by 0.19 eV, in full agreement with all the experimental data.

The optimised geometry of **4**$^+$ is very close to that found in the X-ray crystal structure, with the DFT Fe–P separations being slightly longer, as usually observed when non-local corrections are applied. On the other hand, the optimised geometry provides a much accurate location of hydrogen atom than the X-ray data. From this point of view, it is noteworthy that, in the X-ray molecular structure of the related *trans*-$[Cp^*Fe(dippe)(H)_2]^+$complex [17], the hydrogen metrical data are close to those found by DFT on *trans*-$[Cp^*Fe(dppe)(H)_2]^+$.

4. Concluding remarks

We report in this article on the isolation of both the classical ($\mathbf{4}^+$) and non-classical ($\mathbf{2}^+$) dihydride iron complexes, as an illustration of the subtle balance of the steric and electronic environments around the metal in the Cp*Fe(dppe) framework. The dihydrogen derivative $\mathbf{2}^+$ accommodates a slightly elongated dihapto-H_2 ligand, as inferred from T_1 and J_{HD} data, thus suggesting an efficient back-bonding from the metal centre. Despite the fine tuning of the metal π-donor ability, no dihydride/dihydrogen equilibrium is observed. The dihydrogen derivative $\mathbf{2}^+$ transforms irreversibly into its thermodynamically more stable *trans* iron(IV) dihydride isomer $\mathbf{4}^+$, which has been characterised by a X-ray crystal structure. The DFT calculations on the $[CpFe(dpe)H_2]^+$ model and the real $[Cp^*Fe(dppe)H_2]^+$ systems nicely corroborate the experimental data and show the sensitivity of the coordinated dihydrogen ligand to variations of the electron density on the metal.

. Supplementary material

Crystallographic data (excluding structure factors) have been deposited with the Cambridge Crystallographic Data Centre as supplementary publication No. SUP CCDC 166568. Copies of the data can be obtained free of charge on application to the Director, CCDC, 12 Union Road, Cambridge CB2 1EZ, UK; fax: 44 + (1223) 336-033; e-mail: deposit@ccdc.cam.ac.uk.

Acknowledgements. We thank Dr S. Sabo-Étienne (Toulouse) for stimulating discussions and Dr S. Sinbandhit (Rennes) for helpful NMR assistance. Financial support from the French 'Centre national de la recherche scientifique' (CNRS) and of Université de Rennes-1 is acknowledged. Computing facilities were provided by the 'Centre de ressources informatiques' (CRI) of Rennes and the 'Institut de développement et de ressources en informatique scientifique' (IDRIS) of the CNRS.

References

[1] Kubas G.J., Ryan R.R., Swanson B.I., Vergamini P.J., Wasserman H.J., J. Am. Chem. Soc. 106 (1984) 451.
[2] Kubas G.J., Acc. Chem. Res. 21 (1988) 120.
[3] Sabo-Étienne S., Chaudret B., Coord. Chem. Rev. 178–180 (1998) 381.
[4] Heinekey D.M., Oldham W.J. Jr., Chem. Rev. 93 (1993) 913.
[5] Crabtree R.H., Angew. Chem. Int. Ed. Engl. 32 (1993) 789.
[6] Jessop P.G., Morris R.H., Coord. Chem. Rev. 121 (1992) 155.
[7] Crabtree R.H., Acc. Chem. Res. 23 (1990) 95.
[8] Maseras F., Lledós A., Clot E., Eisenstein O., Chem. Rev. 100 (2000) 601 and references therein.
[9] Toupadakis A., Kubas G.J., King W.A., Scott B.L., Huhmann-Vincent J., Organometallics 17 (1998) 5315.
[10] Heinekey D.M., Radzewich C.E., Voges M.H., Schomber B.M., J. Am. Chem. Soc. 119 (1997) 4172.
[11] Heinekey D.M., Voges M.H., Barnhart D.M., J. Am. Chem. Soc. 118 (1996) 10792.
[12] Castellanos A., Ayllon J.A., Sabo-Étienne S., Donnadieu B., Chaudret B., Yao W.B., Kavallieratos K., Crabtree R.H., C. R. Acad. Sci. Paris, Ser. IIc 2 (1999) 359.
[13] Chinn M.S., Heinekey D.M., J. Am. Chem. Soc. 112 (1990) 5166.
[14] Jia G., Morris R.H., J. Am. Chem. Soc. 113 (1991) 875.
[15] Klooster W.T., Koetzle T.F., Jia G., Fong T.P., Morris R.H., Albinati A., J. Am. Chem. Soc. 116 (1994) 7677.
[16] Hamon P., Toupet L., Hamon J.R., Lapinte C., Organometallics 11 (1992) 1429.
[17] Jimenez-Tenorio M., Puerta M.C., Valerga P., Organometallics 13 (1994) 3330.
[18] Scharrer E., Chang S., Brookhart M., Organometallics 14 (1995) 5686.
[19] Conroy-Lewis F.M., Simpson S.J., J. Chem. Soc. Chem. Commun. (1987) 1675.
[20] Hay P.J., Phys. Lett. 103 (1984) 466.
[21] Saillard J.Y., Hoffmann R., J. Am. Chem. Soc. 106 (1984) 2006.
[22] Sabo-Étienne S., Rodriguez V., Donnadieu B., Chaudret B., El-Makarim H.A., Barthelat J.C., Ulrich S., Limbach H.H., Moise C., New J. Chem. 25 (2001) 55.
[23] Roger C., Hamon P., Toupet L., Rabaâ H., Saillard J.Y., Hamon J.R., Lapinte C., Organometallics 10 (1991) 1045.
[24] Hamon P., Toupet L., Hamon J.R., Lapinte C., Organometallics 15 (1996) 10.
[25] Hamilton D.G., Crabtree R.H., J. Am. Chem. Soc. 110 (1988) 4126.
[26] Van Geet A.L., Anal. Chem. 42 (1970) 679.
[27] Spek A.L., HELENA, Program for the handling of CAD4-Diffractometer Output SHELX(S/L), Utrecht University, Utrecht, The Netherlands, 1997.
[28] Altomare A., Burla M.C., Camalli M., Cascarano G., Giacovazzo C., Guagliardi A., Moliterni A.G.G., Polidori G., Spagna R., J. Appl. Chem. 31 (1998) 74.
[29] Sheldrick G.M., SHELX97, Program for the refinement of crystal structures, University of Göttingen, Götingen, Germany, 1997.
[30] International Tables for X-ray Crystallography, Kluwer Academic Publishers, Dordrecht, vol. C, 1992.
[31] Spek A.L., PLATON-98, A Multipurpose Crystallographic Tool, Utrecht University, Utrecht, The Netherlands, 1998.
[32] Baerends E.J., Ellis D.E., Ros P., Chem. Phys. 2 (1973) 41.
[33] Baerends E.J., Ros P., Int. J. Quantum Chem. S12 (1978) 169.
[34] Boerrigter P.M., te Velde G., Baerends E.J., Int. J. Quantum Chem. 33 (1988) 87.
[35] te Velde G., Baerends E.J., J. Comput. Phys. 99 (1992) 84.
[36] Amsterdam Density Functional (ADF) program, version 2.3, Vrije Universiteit, Amsterdam, The Netherlands, 1996.
[37] Vosko S.D., Wilk L., Nusair M., Can. J. Chem. 58 (1990) 1200.
[38] Becke A.D., J. Chem. Phys. 84 (1986) 4524.
[39] Becke A.D., Phys. Rev. A 38 (1988) 3098.
[40] Perdew J.P., Phys. Rev. B 33 (1986) 8882.
[41] Perdew J.P., Phys. Rev. B 34 (1986) 7406.
[42] Verluis L., Ziegler T.J., Chem. Phys. 88 (1988) 322.
[43] Ziegler T., Rauk A., Theor. Chim. Acta. 46 (1977) 1.
[44] Ziegler T., J. Am. Chem. Soc. 105 (1983) 7543.
[45] Ziegler T., Tschinke V., Becke A., Polyhedron 6 (1987) 685.
[46] Maltby P.A., Schlaf M., Steinbeck M., Lough A.J., Morris R.H., Klooster W.T., Koetzle F.T., Srivastava R.C., J. Am. Chem. Soc. 118 (1996) 5396.

[47] Luther T.A., Heinekey D.M., Inorg. Chem. 37 (1998) 127.
[48] Crabtree R.H., Lavin M., J. Chem. Soc. Chem. Commun. (1985) 1661.
[49] Bautista M.T., Earl K.A., Maltby P.A., Morris R.H., Schweitzer C.T., Sella A., J. Am. Chem. Soc. 110 (1988) 7031.
[50] Earl K.A., Jia G., Maltby P.A., Morris R.H., J. Am. Chem. Soc. 113 (1991) 3027.
[51] Paul F., Lapinte C., Coord. Chem. Rev. 178–180 (1998) 427.
[52] Tilset M., Fjeldahl I., Hamon J.R., Hamon P., Toupet L., Saillard J.Y., Costuas K., Haynes A., J. Am. Chem. Soc. 123 (2001) 9984.
[53] Paciello R.A., Manriquez J.M., Bercaw J.E., Organometallics 9 (1990) 260.
[54] Morris R.H., Inorg. Chem. 31 (1992) 1471.
[55] Hamon P., Hamon J.R., Lapinte C., unplublished work.
[56] Asirvatham V.S., Yao Z., Klabunde K.J., J. Am. Chem. Soc. 116 (1994) 5493.
[57] Yao Z.G., Klabunde K.J., Asirvatham A.S., Inorg. Chem. 34 (1995) 5289.
[58] Yao Z.G., Klabunde K.J., Organometallics 14 (1995) 5013.
[59] Yao Z.G., Klabunde K.J., Hupton A.C., Inorg. Chim. Acta 259 (1997) 119.
[60] Gusev D.G., Hubener R., Burger P., Orama O., Berke H., J. Am. Chem.Soc. 119 (1997) 3716.
[61] Ruiz J., Astruc D., Bideau J.P., Cotrait M., Acta Crystallogr. C 46 (1990) 2367.
[62] Krueger S.T., Poli R., Rheingold A.L., Staley D.L., Inorg. Chem. 28 (1989) 4599.
[63] Cummins C.C., Schrock R.R., Inorg. Chem. 33 (1994) 395.
[64] Vancaemelbecke E., Will S., Autret M., Adamian V.A., Lex J., Gisselbrecht J.P., Gross M., Vogel E., Kadish K.M., Inorg. Chem. 35 (1996) 184.
[65] Li M., Shang M.Y., Ehlinger N., Schulz C.E., Scheidt W.R., Inorg. Chem. 39 (2000) 580.
[66] Pasek E.A., Straub D.Y., Inorg. Chem. 11 (1972) 259.
[67] Coucouvanis D., Hollander F.J., Pedelty R., Inorg. Chem. 16 (1977) 2691.
[68] Sellmann D., Emig S., Heinemann F.W., Angew. Chem. Int. Ed. Engl. 36 (1997) 1734.
[69] Desbois M.H., Astruc D., Angew. Chem. Int. Ed. Engl. 28 (1989) 460.
[70] Bower B.K., Tennent H.G., J. Am. Chem. Soc. 94 (1972) 2512.
[71] Jetz W., Graham W.A.G., Inorg. Chem. 10 (1971) 1159.
[72] Manojlovic-Muir L., Muir K.W., Ibers J.A., Inorg. Chem. 9 (1970) 447.
[73] Schubert U., Gilbert S., Mock S., Chem. Ber. 125 (1992) 835.